Journal of Virology

Superinfection Exclusion in Alphabaculovirus Infections Is Concomitant with Actin Reorganization

Inés Beperet, Sarah L. Irons, Oihane Simón, Linda A. King, Trevor Williams, Robert D. Possee, Miguel López-Ferber and Primitivo Caballero

J. Virol. **2014, 88(6):3548. DOI: 10.1128/JVI.02974-13.**
Published Ahead of Print 8 January 2014.

JVI Journals.ASM.org

Superinfection Exclusion in Alphabaculovirus Infections Is Concomitant with Actin Reorganization

Inés Beperet,[a,b] Sarah L. Irons,[b] Oihane Simón,[a] Linda A. King,[b] Trevor Williams,[c] Robert D. Possee,[d] Miguel López-Ferber,[e] Primitivo Caballero[a,f]

Bioinsecticidas Microbianos, Instituto de Agrobiotecnología, CSIC-UPNA, Gobierno de Navarra, Mutilva Baja, Navarra, Spain[a]; Department of Biological and Medical Sciences, Faculty of Health and Life Sciences, Oxford Brookes University, Oxford, United Kingdom[b]; Instituto de Ecología AC, Xalapa, Veracruz, Mexico[c]; Centre for Ecology and Hydrology, Crowmarsh Gifford, Wallingford, Oxfordshire, United Kingdom[d]; LGEI, Ecole des Mines d'Alès, Alès, France[e]; Departamento de Producción Agraria, Universidad Pública de Navarra, Pamplona, Navarra, Spain[f]

ABSTRACT

Superinfection exclusion is the ability of an established virus to interfere with a second virus infection. This effect was studied *in vitro* during lepidopteran-specific nucleopolyhedrovirus (genus *Alphabaculovirus*, family *Baculoviridae*) infection. Homologous interference was detected in Sf9 cells sequentially infected with two genotypes of *Autographa californica* multiple nucleopolyhedrovirus (AcMNPV), each one expressing a different fluorescent protein. This was a progressive process in which a sharp decrease in the signs of infection caused by the second virus was observed, affecting not only the number of coinfected cells observed, but also the level of protein expression due to the second virus infection. Superinfection exclusion was concurrent with reorganization of cytoplasmic actin to F-actin in the nucleus, followed by budded virus production (16 to 20 h postinfection). Disruption of actin filaments by cell treatment with cytochalasin D resulted in a successful second infection. Protection against heterologous nucleopolyhedrovirus infection was also demonstrated, as productive infection of Sf9 cells by *Spodoptera frugiperda* nucleopolyhedrovirus (SfMNPV) was inhibited by prior infection with AcMNPV, and vice versa. Finally, coinfected cells were observed following inoculation with mixtures of these two phylogenetically distant nucleopolyhedroviruses—AcMNPV and SfMNPV—but at a frequency lower than predicted, suggesting interspecific virus interference during infection or replication. The temporal window of infection is likely necessary to maintain genotypic diversity that favors virus survival but also permits dual infection by heterospecific alphabaculoviruses.

IMPORTANCE Infection of a cell by more than one virus particle implies sharing of cell resources. We show that multiple infection, by closely related or distantly related baculoviruses, is possible only during a brief window of time that allows additional virus particles to enter an infected cell over a period of ca. 16 h but then blocks multiple infections as newly generated virus particles begin to leave the infected cell. This temporal window has two important consequences. First, it allows multiple genotypes to almost simultaneously infect cells within the host, thus generating genetically diverse virus particles for transmission. Second, it provides a mechanism by which different viruses replicating in the same cell nucleus can exchange genetic material, so that the progeny viruses may be a mosaic of genes from each of the parental viruses. This opens a completely new avenue of research into the evolution of these insect pathogens.

Superinfection exclusion is a mechanism by which a virus that establishes an infection in a host excludes subsequent infection by another virus (1–3). This effect has generally been examined using homologous interference, in which the mechanism of exclusion acts against the same or a closely related virus (4, 5). Superinfection exclusion prevents competition by protecting the first infecting virus from competitors even if the first infecting virus is the weaker competitor overall. This allows the first virus to maximize the production of progeny virus particles once the cell has been infected. Although superinfection exclusion is a recognized effect for different virus species, several mechanisms for the phenomenon have been described (2, 3, 6–8). However, total exclusion brings potential disadvantages for the virus, as it reduces or abolishes the possibility of generation of recombinants in situations in which the generation of genetic diversity is advantageous for virus survival.

Superinfection exclusion has previously been described in the family *Baculoviridae* (9–11), although the mechanism underlying the process remains unclear. Members of this family of occluded, double-stranded DNA viruses have proved remarkably valuable as pest control agents (12), as protein expression systems (13–16), for vaccine production (17, 18), and as potential therapeutic gene delivery vectors (19). Members of the genus *Alphabaculovirus* infect lepidopteran insects through host consumption of plant material contaminated by virus-containing occlusion bodies (OBs). The OB breaks down in the insect midgut, releasing occlusion-derived virions (ODVs) that infect midgut cells by fusion with the epithelial cell membrane, a process that involves a number of per-oral infection factors (20, 21). Following an initial infection cycle, budded virions (BV) that bud through the basal membrane of the

Received 18 October 2013 **Accepted** 1 January 2014
Published ahead of print 8 January 2014
Editor: G. McFadden
Address correspondence to Miguel López-Ferber, miguel.lopez-ferber@mines-ales.fr.

doi:10.1128/JVI.02974-13

cell are produced. These progeny initiate secondary infections that disseminate the virus throughout the host insect. The secondary infection process starts when a budded virion enters a susceptible cell by endocytosis (22), a process that is mediated by a specific virion protein, GP64. Budded virus nucleocapsids are then released from endosomes and move rapidly to the cell nucleus, where virus replication begins (23, 24). Newly synthesized viral DNA is assembled into nucleocapsids, with two virion phenotypes produced during the course of infection: initially, nucleocapsids are transported to the cell periphery and bud out of cells as budded virions, whereas later in infection, nucleocapsids are retained in the nucleus and acquire a membrane synthesized *de novo*, forming ODVs that are subsequently occluded in a polyhedrin protein matrix to form OBs (24). A functional cytoskeleton is required for virus entry and egress during the infection cycle (23, 25, 26). Actin has been suggested to be of key importance during viral transportation to the nucleus, gene expression, and viral progeny production (23, 27, 28). For example, treatment of baculovirus-infected cells with cytochalasin D (CD), a drug that inhibits actin polymerization, results in a lack of localization of F-actin and newly synthesized nucleocapsids, and this inhibits the production of virus progeny (29, 30). In contrast, microtubules have been demonstrated to be important in anterograde trafficking of nucleocapsids from the nucleus to the membrane for the production of budded virions (25).

In the present study, we characterized superinfection exclusion in alphabaculoviruses using two recombinant genotypes of *Autographa californica* multiple nucleopolyhedrovirus (AcMNPV) that differed in the expression of fluorescent proteins as a tool to study homologous interference and the role of actin in the superinfection exclusion process. We went on to characterize superinfection exclusion in a heterologous virus system involving AcMNPV and a phylogenetically distant alphabaculovirus, *Spodoptera frugiperda* MNPV (SfMNPV) (31). The results obtained in this study give new insights into the alphabaculovirus infection process and the existence of competition between viruses.

MATERIALS AND METHODS

Cell line and viruses. The Sf9 cell line, a clonal isolate of *S. frugiperda* Sf21 cells, was maintained at 28°C in TC100 medium supplemented with 10% (vol/vol) fetal calf serum (32). AcEGFP-PH$^+$ and AcdsRed-PH$^+$ were kindly provided by Caroline Griffiths, Oxford Brookes University. Both recombinant viruses have the respective fluorescent protein (enhanced green fluorescent protein [EGFP] or dsRed)-encoding gene inserted into the *polyhedrin* locus under the control of the *polyhedrin* promoter and the *polyhedrin* gene inserted into the *p10* locus under the control of the *p10* promoter in the AcMNPV-C6 genome, resulting in an occlusion-positive virus (33). AcEGFP-PH$^-$ virus was kindly provided by John O. Danquah, Oxford Brookes University. The *egfp* gene is inserted into the *polyhedrin* locus under the control of the *polyhedrin* promoter in this virus, resulting in an occlusion-negative virus. The SfMNPV used in this study was a plaque-purified variant (genotype B) of a Nicaraguan isolate of SfMNPV (34). All viruses were propagated in Sf9 cells at 28°C using standard methods (32).

Analysis of superinfection exclusion against a homologous virus. Sequential infections of Sf9 cells were performed at different time intervals using budded virions of AcEGFP-PH$^+$ and AcdsRed-PH$^+$. For this, 1×10^6 cells were seeded onto sterile glass coverslips in 35-mm dishes and were allowed to settle at room temperature for 2 h. Infections were performed by removing the medium and adding 100 μl of the first virus (at 10^8 PFU/ml) at a multiplicity of infection (MOI) of 10, which ensured synchronous infection. Virions were allowed to adsorb for 1 h at room temperature; the inoculum was then replaced by fresh medium, and the cells were incubated at 28°C. A total of six infection treatments were performed (Fig. 1 shows a schematic experimental plan: mock-infected cells [A], cells infected with AcEGFP-PH$^+$ alone [B], cells infected with AcdsRed-PH$^+$ alone [C], simultaneous inoculation with both viruses [MOI = 10 AcEGFP-PH$^+$ + 10 AcdsRed-PH$^+$] [D], sequential inoculation with AcEGFP-PH$^+$ as the first virus and AcdsRed-PH$^+$ as the second virus [E], and cells inoculated with AcdsRed-PH$^+$ at the same time as second inoculations were performed in treatment E [F]). Superinfection exclusion effects were detected by comparing each virus signal in sequentially inoculated samples (Fig. 1E) to that of the respective controls (Fig. 1B and F). AcdsRed-PH$^+$ infections in superinfection samples (Fig. 1E) and superinfection controls were performed at 3, 6.5, 9.5, 13, 16, 24, 27, 30.5, 38, 43, and 48 h after the first infection (h p.i.) following the same method described for the first infection. Time point zero for the whole experiment was considered to be the moment at which the first virus

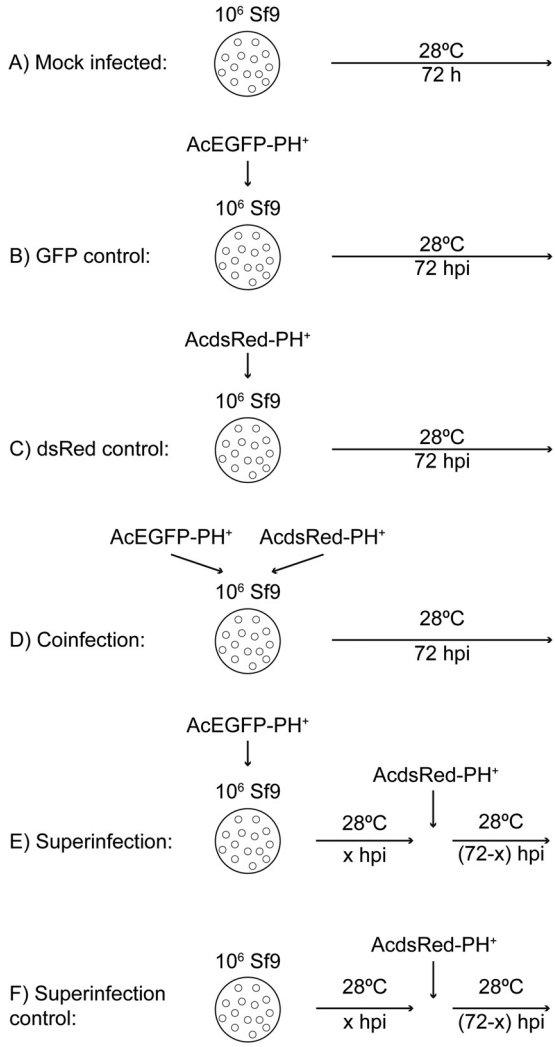

FIG 1 Schematic representation of the first superinfection exclusion experiment, in which Sf9 cells were mock-infected controls (A), inoculated once with AcEGFP$^-$PH$^+$ (B), inoculated once with AcdsRed-PH$^+$ (C), inoculated simultaneously with both viruses (D), inoculated initially with AcEGFP-PH$^+$ and subsequently with AcdsRed-PH$^+$ (E), or inoculated initially with AcdsRed-PH$^+$ and subsequently with AcEGFP-PH$^+$ (F). (B to E) In all cases, the cells were incubated at 28°C for 72 h following the first inoculation (time point zero). (F) In the complementary experiment, the order of virus inoculation was inverted.

inoculum was added to the set of cells from treatments in Fig. 1B, C, D, and E. At 72 h, the cells were fixed with freshly prepared 4% paraformaldehyde (PFA) in phosphate-buffered saline (PBS) for 20 min at room temperature. The cells on the coverslip were then washed twice with PBS and mounted in Vectashield fluorescence microscopy aqueous mounting medium (Vector Laboratories). Confocal images were acquired with a Zeiss LSM 510 microscope and processed with LSM Image Browser (Zeiss). At least two images were taken for each sample, and each infection was performed in duplicate. Image acquisition settings were identical for all images. Red cells (AcdsRed-PH$^+$ infected), green cells (AcEGFP-PH$^+$ infected), and cells with the presence of both colors (dually infected cells) were counted for each image. Expression of the red fluorescent protein was also estimated by quantifying the fluorescence intensities of 10 randomly selected cells per image following the subtraction of the background level in both superinfection and superinfection control samples using Scion Image software (Scion Corporation). The fluorescence intensity measurements were averaged for each replicate and were compared at each time point by *t* test using SPSS v.15 (SPSS Inc., Chicago, IL).

Budded virus production. The titer of budded virus in the medium was studied to determine the temporal relationship between the exit of virions from infected cells and the development of the exclusion process. For this, batches of 10^6 Sf9 cells were seeded and infected at an MOI of 10 with AcEGFP-PH$^+$ virus, as previously described. The medium was collected at different times (0, 1, 3, 6.5, 9.5, 13, 16, 20, 24, 27, 30, 38, 48, and 72 h p.i.) and centrifuged at 2,000 × *g* to pellet the cells. DNA extraction was then performed on each supernatant fraction using the MasterPure Complete DNA Purification kit (Epicentre Biotechnologies). Viral genomic DNA was quantified using quantitative PCR (qPCR) based on SYBR green fluorescence in an ABI Prism 7900HT Sequence Detection System (Applied Biosystems). Specific primers were used to amplify in the unique gene *ac97* of AcMNPV (Ac.1, GATTTGTTGGCCGAATAACG; Ac.2, TG ACTCTTTCACCCATTGCAG). The resulting PCR product was cloned into the pGEM-T Easy vector (Promega). Known dilutions of plasmid DNA were used as internal standards for qPCR. The reaction mixture (20 μl) contained 10 μl SYBR Premix *Ex Taq* (2×), 0.4 μl of ROX reference dye (50×), 0.2 μl of each primer (10 pmol/μl), and 1 μl of DNA template. qPCR was performed under the following conditions: 95°C for 30 s, followed by 45 amplification cycles of 95°C for 5 s and 60°C for 30 s, and finally, a dissociation stage of 95°C for 15 s, 60°C for 15 s, and 95°C for 15 s. All reactions were performed in triplicate. Data acquisition and analysis were handled by Sequence Detector version 2.2.2 software (Applied Biosystems). Melting-curve analysis was performed to confirm specific replicon formation during qPCR. The entire experiment was performed in triplicate.

Effect of blocking actin polymerization on superinfection exclusion. To examine the effect of CD treatment on superinfection exclusion, batches of 10^6 Sf9 cells were seeded and infected with the AcEGFP-PH$^+$ virus as previously described. The virus was then replaced by medium containing 5 μg/ml of CD in 0.1% dimethyl sulfoxide (DMSO). At 24 h p.i., a second infection with AcdsRed-PH$^+$ virus was performed. At that moment, the virus inoculum was replaced by medium in half of the samples, whereas in the other half, it was replaced by CD-containing medium. Mock-infected cells were set up as controls, as described for superinfection exclusion above, as well as AcdsRed-PH$^+$-alone and AcEGFP-PH$^+$-alone treatments (Fig. 1A, B, C, and F), each with and without CD treatment. Also, two batches of 10^6 cells were inoculated with AcEGFP-PH$^+$ and reinoculated 24 h later with AcdsRed-PH$^+$ in the absence of CD treatment as an exclusion control (Fig. 1E). Control cultures without CD were treated with 0.1% DMSO. Time point zero for the whole experiment was considered to be the moment at which the first virus inoculum was added to the samples that would subsequently be subjected to superinfection at intervals. At 48 h, the drug and the medium containing DMSO were removed, the cells were rinsed twice with medium, and fresh medium was added. Twenty-four hours later, the cells were fixed as previously described. The experiment was performed in triplicate. Confocal images were acquired with a Nikon D-Eclipse C1 microscope and processed with EZ-C1 software (Nikon).

Exclusion against heterologous viruses. Batches of 4×10^5 cells/well were seeded onto sterile glass coverslips in 12-well plates and were allowed to settle at room temperature for 2 h. The cells were then inoculated with 80 μl of a 5×10^7 PFU/ml concentration of virus (MOI = 10) to ensure a synchronous infection. To determine exclusion against a heterologous virus, the cells were first inoculated with the polyhedrin-negative virus AcEGFP-PH$^-$. The virus was allowed to adsorb for 1 h at room temperature; the virus inoculum was then replaced with fresh medium, and the cells were incubated at 28°C for 24 h. These cells were then inoculated with SfMNPV budded virions (MOI = 10), as previously described. The cells were incubated for another 48 h at 28°C (a total of 72 h following the first inoculation). Overall, four different treatments were performed: (i) inoculation of cells with AcEGFP-PH$^-$, followed 24 h later by inoculation with SfMNPV; (ii) a simultaneous infection in which both viruses were present in the same inoculum (MOI = 10 + 10); (iii) an AcEGFP-PH$^-$ treatment in which cells were inoculated with the virus alone at time point zero; and (iv) an SfMNPV treatment, in which cells were inoculated with SfMNPV alone 24 h after the start of the experiment. Time point zero for the whole experiment was considered to be the moment at which the first virus inoculum was added to the cells in treatment i. Seventy-two hours later, the cells were fixed and images were acquired with the confocal microscope. Cells infected with AcEGFP-PH$^-$ were identified by the presence of green fluorescence, whereas cells infected by SfMNPV were identified by the presence of OBs. The presence of green fluorescence and OBs in the same cell was used as an indicator of dual infection by both viruses. Furthermore, the ability of SfMNPV to establish superinfection exclusion was also tested by performing an identical set of treatments in which SfMNPV was inoculated first, followed 24 h later by inoculation with AcEGFP-PH$^-$, as previously described.

Finally, 10 batches of cells were infected simultaneously with mixtures of AcEGFP-PH$^-$ and SfMNPV (MOI = 10 + 10), as previously described, to test for the presence of interactions between these viruses during the early stages of the infection process. At 72 h p.i., the cells were fixed and confocal images were acquired. Cells infected by each virus alone, dually infected cells, and the total cells in each image were counted.

Statistical analysis. The probabilities of infection were calculated according to the Poisson distribution, with a mean (λ) of 10 (i.e., the MOI). The probability of a cell being dually infected by at least one virion of each virus was calculated as follows: $1 - P_{AB} - P_A - P_B$, where P_{AB} is the probability of escaping infection by either virus (2.06×10^{-9}), P_A is the probability of infection with virus A alone (4.54×10^{-4}), and P_B is the probability of infection with virus B alone (4.54×10^{-4}). For an MOI of 10 for each virus, this calculation indicates that >99.9% of cells would be dually infected, assuming that all cells were equally susceptible to infection at the moment of inoculation and that all virions were equally infectious.

The prevalence of dual infection was estimated as the product of the proportion of SfMNPV-infected cells and the proportion of AcEGFP-PH$^-$-infected cells. This product was taken as the expected prevalence of dual infection, assuming that viruses do not interfere with one another during the early stages of infection, prior to the appearance of OBs or fluorophore protein. The proportions of observed and expected dually infected cells were compared by a paired *t* test after fitting a generalized linear model in GLIM with a binomial error structure specified (35).

RESULTS

Superinfection exclusion based on homologous interference depends on the time lag between infections. To investigate the temporal aspects of superinfection exclusion, an initial infection with AcMNPV expressing EGFP was followed at different time points with a second infection challenge from AcMNPV bearing dsRed. The process of infection and exclusion was quantified by measurement of fluorescence intensities in infected cells. No significant differences were observed in the numbers of cells infected

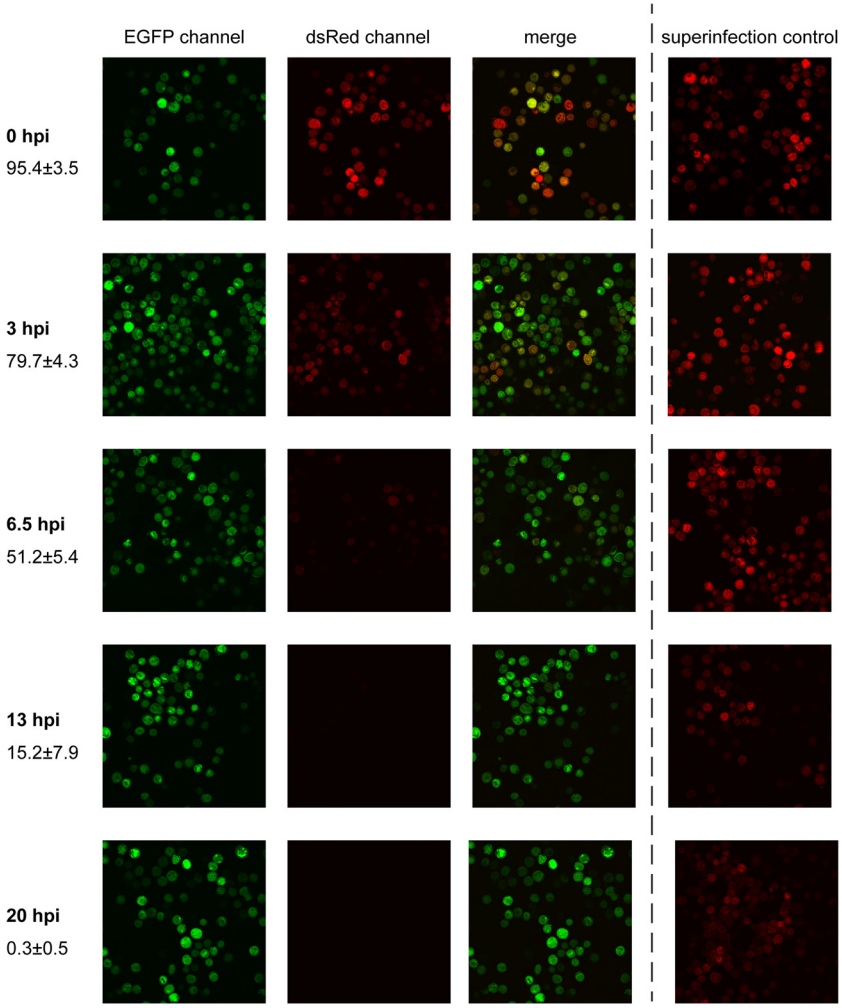

FIG 2 The degree of superinfection was directly affected by the time interval between the initial and second infections. Shown are confocal images of samples of superinfections at different times and their respective controls. The EGFP channel and the dsRed channel show AcEGFP-PH$^+$-infected cells and AcdsRed-PH$^+$-infected cells in the superinfection samples (Fig. 1E), respectively. The merged image of the EGFP and dsRed channels (merge) shows coinfected cells in various shades of yellow depending on the relative expression of GFP and dsRed. The superinfection control images represent AcdsRed-PH$^+$-only-infected cells (Fig. 1F) as a control for the second virus infection. The numbers in boldface correspond to the time interval between inoculations (h p.i.), and the numerical values indicate the percentages (±standard deviations [SD]) of coinfected cells with respect to AcEGFP-PH$^+$-infected cells.

with AcEGFP-PH$^+$ or AcdsRed-PH$^+$ viruses following simultaneous inoculation of cells with both viruses. Overall, 4.4% ± 1.2% of cells expressed only the red marker and 3.5% ± 2.1% of cells expressed only the green fluorescent marker. Overall, 95.4% ± 3.5% of infected cells showed expression of both markers, with respect to the frequency of AcEGFP-PH$^+$-infected cells (Fig. 2). The frequency of dual infections decreased with increasing intervals between virus inoculations ($F_{9,51} = 65.94$; $P < 0.001$) (Fig. 2). During the 9.5-h interval between inoculations, increased variability in the frequency of dual infection between replicates was observed and quantified by capturing 13 images at each time point, which were analyzed to estimate dual infection. During the 13- and 16-h intervals between inoculations, less than 20% dually infected cells were observed. During the 20- and 24-h intervals between inoculations, the frequency of dual infection by visual examination of treated cells was <0.5%. Thereafter, no coinfected cells were detected, whereas dsRed emission was clear in the cells that had been treated only with AcdsRed-PH$^+$ at all time points. The complementary experiment was also performed, with AcdsRed-PH$^+$ as the first virus and AcEGFP-PH$^+$ as the second virus, and nearly identical results were observed (Fig. 3).

Resistance to a second virus infection was analyzed by quantification of the fluorescent protein encoded in the second virus genome. Mean fluorescence intensity measurements of red cells estimated with Scion Image software differed significantly between images taken from superinfection samples and superinfection controls at every time point, except from time point zero (Fig. 4). When cells were coinfected, the intensity of AcdsRed-PH$^+$ dsRed fluorescence in superinfection samples was similar to that of the dsRed control samples ($t = 0.359$; df = 3; $P = 0.743$). At the remaining time points, the dsRed expression level decreased in both types of samples, but fluorescence decreased more markedly and was consistently lower in superinfection samples than in the controls treated with single viruses (t test following logarithmic normalization: $t = 2.638$; df = 31; $P = 0.013$). The decreased expression of dsRed in the control samples was likely because the

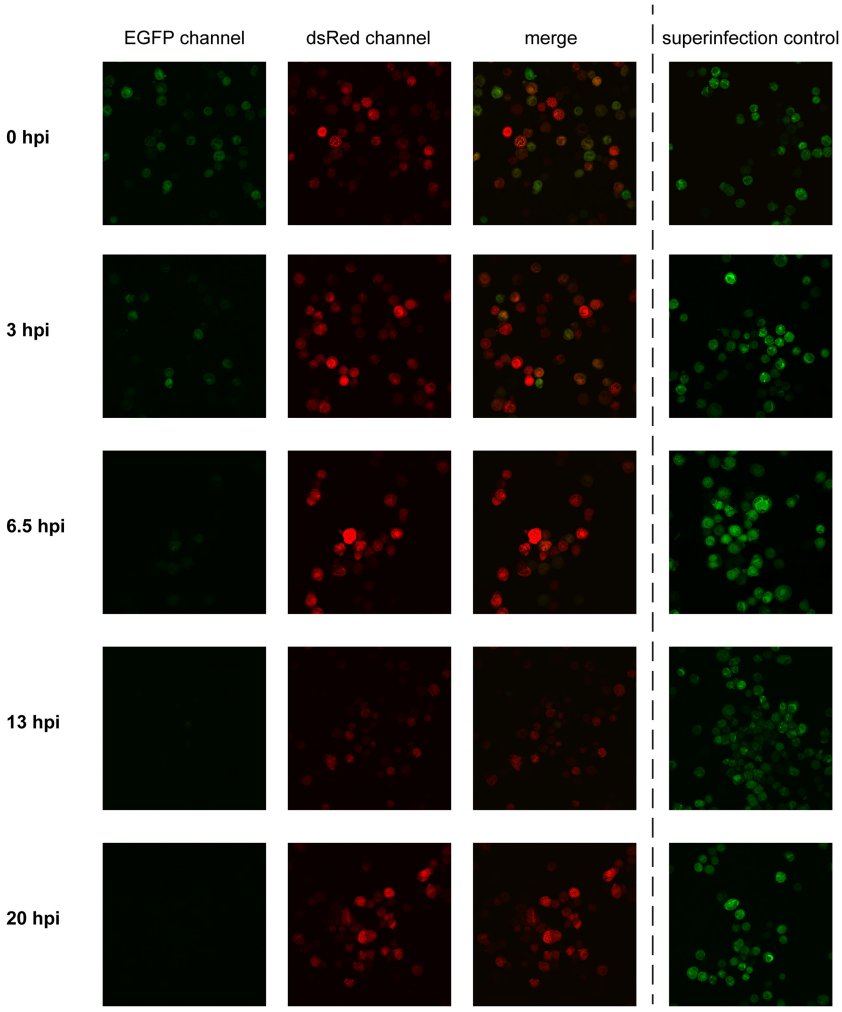

FIG 3 Complementary experiment performed with AcdsRed-PH$^+$ as the first virus and AcEGFP-PH$^+$ as the second inoculum. The scheme is similar to that shown in Fig. 2. The dsRed channel and the EGFP channel show AcdsRed-PH$^+$-infected cells and AcEGFP-PH$^+$-infected cells in the superinfection samples, respectively. The merged image of the dsRed and EGFP channels (merge) shows coinfected cells in various shades depending on the relative expression of GFP and dsRed. The superinfection control images represent AcEGFP-PH$^+$-only-infected cells as a control for the second virus infection. The numbers in boldface correspond to the time interval (h p.i.) between inoculations.

interval between the second infection and fixation was half that of the earlier infection, i.e., AcdsRed-PH$^+$ infection performed 24 h after inoculation with AcEGFP-PH$^+$ in the superinfection treatment left the dsRed gene just 48 h for replication and expression prior to fixation. As the fluorescence genes are under the control of a late promoter, this period was not sufficient to achieve high levels of dsRed expression.

The release of budded virus begins close to the time at which superinfection exclusion occurs. Budded virus release was estimated by quantifying copies of the unique gene *ac97* in cellular supernatants by qPCR (97% efficiency; $r^2 = 0.9960$). An important increase in budded virus production was observed at 16 h p.i., with an average of $11.0 \times 10^5 \pm 0.7 \times 10^5$ viral copies/ml (Fig. 5). At later times, the total amounts of budded virus present in the supernatant continued to increase steadily and reached $7.20 \times 10^7 \pm 0.85 \times 10^7$ copies/ml at 37 h p.i. (Fig. 5). The percentage of dual infections was dramatically reduced when budded viruses began to egress from infected cells and was undetectable soon after.

Disruption of the actin cytoskeleton impedes superinfection exclusion. To explore potential mechanisms of exclusion, the role of the actin cytoskeleton, which is known to be involved in nucleocapsid entry (23), was investigated through disruption by CD. Treatment with CD resulted in a loss of the characteristic rounded shape of Sf9 cells in both uninfected and AcEGFP-PH$^+$-infected cells (Fig. 6A). After removing the drug, the cells recovered their normal shape, indicating that normal polymerization of actin filaments had been restored. Normal levels of red or green fluorescence signals were observed in cells infected by AcdsRed-PH$^+$ and AcEGFP-PH$^+$, with or without CD treatment (Fig. 6Ba and b). No dsRed signal was observed in the exclusion control, in which cells were inoculated with AcEGFP-PH$^+$ and reinoculated 24 h later with AcdsRed-PH$^+$ in the absence of CD treatment (Fig. 6Bc). However, dsRed signal was present in superinfected cells treated with CD, both when the drug had been rinsed out at 24 h p.i. (Fig. 6Bd) and when it had been present during the entire 48-h p.i. period (Fig. 6Be). These observations indicate that superinfection exclusion was overcome in the presence of the CD treatment.

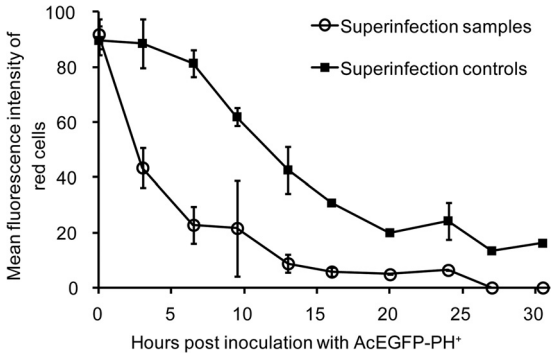

FIG 4 Expression levels of the challenge virus were suppressed in superinfected cells. Shown is a comparison of dsRed expression in terms of the mean relative fluorescence intensity of AcdsRed-PH$^+$-infected cells. Both superinfection samples and superinfection controls were seeded, inoculated with AcdsRed-PH$^+$, incubated, and fixed simultaneously. The only difference was the AcEGFP-PH$^+$ treatment performed in superinfection samples at time zero. Images were taken after fixation at 72 h p.i. The squares indicate the mean relative intensities of red cells in images from superinfection controls (Fig. 1F), and the circles are mean relative intensities of red fluorescence in cells in images from superinfection samples (Fig. 1E). The values in control and superinfection samples differed significantly at every time point after time zero. The error bars represent standard deviations.

Superinfection exclusion is also established against a heterologous alphabaculovirus and is not exclusive to AcMNPV. Having demonstrated that superinfection exclusion occurs between two variants of the same virus, we progressed to studying whether similar responses would occur when different virus species attempted to infect the same cells. When cells were simultaneously inoculated with AcEGFP-PH$^-$ and SfMNPV, both OBs and green fluorescence were simultaneously observed in many of the cells, a clear demonstration of dual infection (Fig. 7A). SfMNPV was not able to establish a productive infection in cells that had been infected 24 h previously with AcEGFP-PH$^-$ (Fig. 7B). Similarly, when the converse experiment was performed using SfMNPV as the first virus, followed 24 h later by AcEGFP-PH$^-$ inoculation, only OBs were observed in the cell nucleus in the absence of cell fluorescence (Fig. 7C). Hence, SfMNPV was able to block subsequent productive infection by AcMNPV.

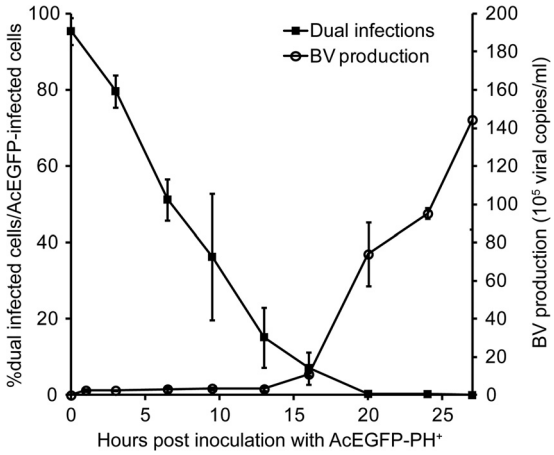

FIG 5 Suppression of superinfection was concurrent with budded virus egress from infected cells. The prevalence of dual infection in cells and BV production varied over time. The error bars indicate standard deviations.

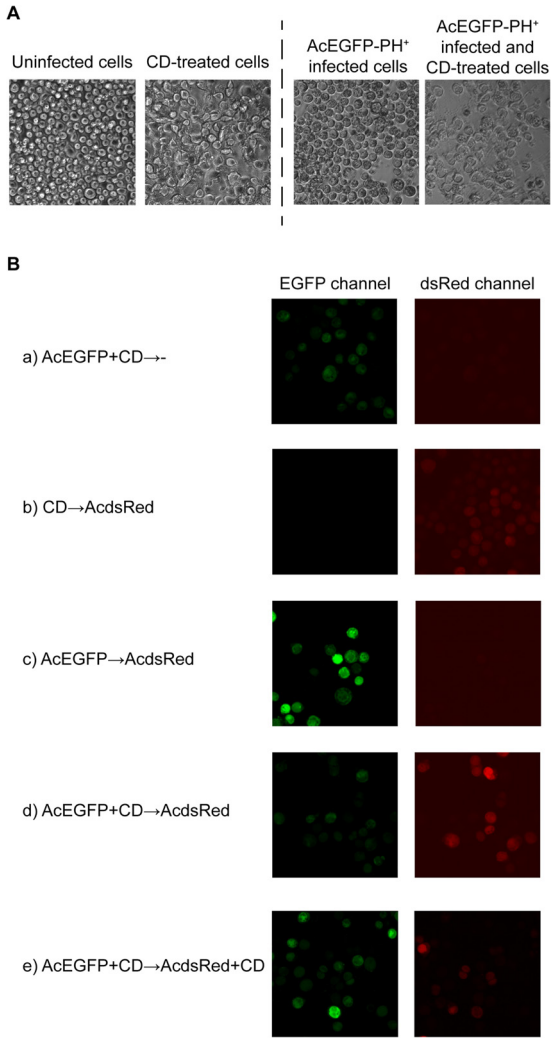

FIG 6 Superinfection exclusion was impeded by actin reorganization. (A) Comparisons between cells treated with CD and untreated cells among both uninfected and AcEGFP-PH$^+$-infected cells. The images were taken at 48 h p.i. (B) Confocal images of superinfection samples treated with CD and untreated cells. The cells for treatments c, d, and e were initially inoculated with AcEGFP-PH$^+$ and subsequently with AcdsRed-PH$^+$. The EGFP channel and the dsRed channel show AcEGFP-PH$^+$-infected cells and AcdsRed-PH$^+$-infected cells, respectively. The arrow in the label for each treatment (a to e) represents the 24-h period elapsed between inoculations. CD was removed at 48 h p.i., except for treatment d, in which CD was removed before the second inoculation. The images were taken at 72 h p.i.

An average (±standard error [SE]) of 132.4 ± 49.2 cells were examined in each replicate, 80.8% ± 4.6% of which showed signs of infection. Overall, 85.8% (SE range, 84.8% to 86.8%) of virus-infected cells were infected by SfMNPV, 14.2% (SE range, 13.2% to 15.1%) were infected by AcEGFP-PH$^-$, and 3.8% (SE range, 3.3% to 4.4%) were infected by both viruses. The expected mean percentage of dual infection across replicates was calculated at 12.2%, which was significantly higher than the observed mean prevalence (3.8%) of dual infection (paired t test; $t = 4.60$; df = 4; $P = 0.01$).

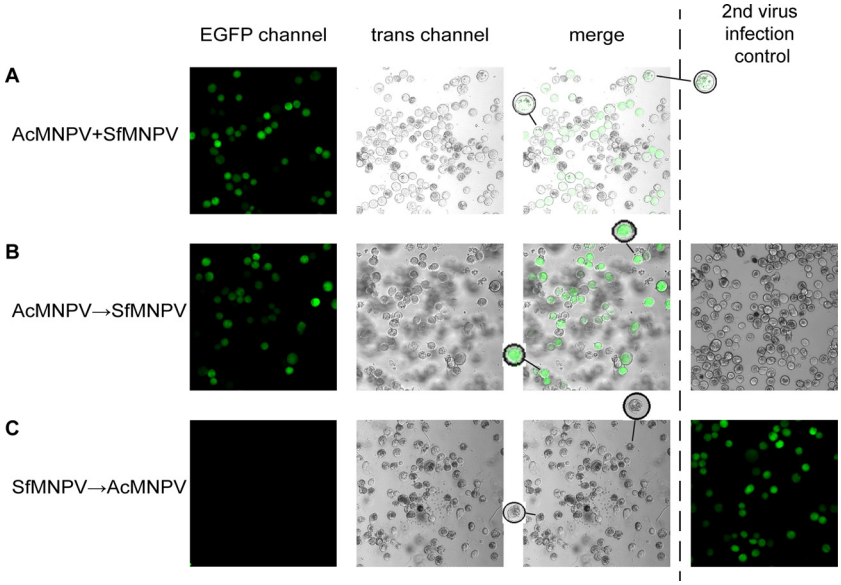

FIG 7 Heterologous interference between different viruses. Sf9 cells were infected with EGFP-expressing AcMNPV and then challenged with SfMNPV immediately (A) or with a 24-h delay (B) or vice versa (C). The EGFP channel shows AcEGFP-PH$^-$-infected cells. SfMNPV-infected cells containing OBs can be visualized on the trans channel. The merge channel presents images following the merger of both channels. The close-ups of cells within circles reveal the presence/absence of OBs and green fluorescence inside the cells. The second virus infection control column shows images of cells infected with SfMNPV alone or AcEGFP-PH$^-$ at the same time that inoculation of the second virus (superinfection) was performed. The arrows in the labels of the treatments indicate cells that were inoculated at an interval of 24 h with both viruses.

DISCUSSION

Superinfection exclusion against a homologous alphabaculovirus was detected by sequentially infecting Sf9 cells with two different genotypes of AcMNPV. The exclusion effect was studied using genotypes carrying different fluorescent-protein genes under the control of very late promoters. Therefore, the presence of the fluorescent signals could be directly related to a complete and successful infection of the respective virus(es). The interval between infections that resulted in a very low frequency ($\leq$1%) of dual infections was 20 h or more. A temporal window similar to that of superinfection was previously reported for occlusion-negative viruses in Sf21 or Sf9 cells using fluorescence microscopy (9, 11).

The block to infection with a second virus was quantified by visual counts of the percentage of dually infected cells and confirmed by analysis of the fluorescence intensity due to fluorophore expression by the second virus, which was consistently lower in the superinfecting virus than in the corresponding single-infection control treatments.

High MOIs have been linked to decreased cell viability in cell culture systems (36), although we observed no noticeable change in cell death kinetics in our study involving an MOI of 10, or up to 20 in dually inoculated cells. Also, cells exposed to high MOIs do not appear to experience saturation of cellular receptors (37–40), even when inocula comprise high titers of defective particles (11). In contrast, MOI values in insect larvae infected by a baculovirus have been estimated at 4 or 5 genomes/cell (41). At this MOI, almost all susceptible cells of the larva will become infected (Poisson estimated probability of not being infected, $P = 0.018$ to 0.007), thus maximizing the exploitation of host cellular resources for the replication of these pathogens. In addition, from ecological and evolutionary perspectives, maintaining a temporal window of susceptibility to superinfection is a mechanism by which genotypically diverse virions can coinfect a single cell, resulting in the production of genotypically heterogeneous OBs (42) that can be more transmissible than genotypically uniform OBs, thereby increasing the probability of survival of the baculovirus population (43, 44).

The cooccurrence of superinfection exclusion with the start of the exit of budded virions from infected cells revealed a temporal link between the two events. Hence, exclusion may be associated with cellular changes that are themselves associated with the egress of budded virions, which occurs at the beginning of the late stage of infection (28). The possibility that the lack of dsRed fluorescent signal may have been due to cell death following the first infection was discounted, as the cells were just beginning full production of budded virions when they became totally refractive to a second infection, which was long before any cytopathic effects were observed (4 to 5 days); apoptosis was also not observed in AcdsRed-PH$^+$-treated cells. Actin filaments have a key role in this transition phase. In the early stages of infection, viral transcription is carried out by the host RNA polymerase II, whereas late and very late viral gene expression is mediated by a virus-encoded RNA polymerase (24, 45, 46). The baculovirus polymerase is actin sensitive (29), and it has been hypothesized that a shift in the nucleus from G-actin to F-actin, which is part of the virogenic stroma and stabilizes the formation of nucleocapsids, is responsible for silencing the host RNA polymerase II (28). Therefore, actin polymerization in the nucleus is likely to be involved in silencing of both host and early viral gene transcription.

Nucleocapsid trafficking to the nucleus is mediated by thick actin filaments in the cytoplasm that interact with the viral P78/83 capsid protein (23). This conformation changes in the following hours (4 to 7 h p.i.), the cytoplasmic cables disappear, and the G-actin concentration increases in the nucleus (28, 47). These

processes are mediated by a number of viral genes, including *arif-1* (23, 48, 49). Nuclear actin polymerizes later in infection (~12 h p.i.), concurrent with the beginning of assembly of progeny nucleocapsids (28, 47). This may be the reason why superinfection from 6 h p.i. onward resulted in lower expression of the second virus in dually infected cells, as during this period, cytoplasmic F-actin is less available to assist the transport of infecting nucleocapsids toward the nucleus and nuclear actin is also in a suboptimal configuration to facilitate host RNA polymerase in early viral gene expression.

As the lag between the first and second infections increases, the degree of virus-induced actin reorganization from the cytoplasm and within the nucleus, specifically, the reduced availability of G-actin, becomes increasingly incompatible with gene expression of the second virus at later times postinfection. In addition, the presence of early gene expression inhibitors from the first infecting virus in the nuclear environment is likely to severely hinder the expression of the early gene set of the second infecting virus. At 16 to 20 h p.i., the cell becomes fully refractive to superinfection and is geared up to budded virus production. At this moment, the second virus was unable to generate a productive infection. Whether the second virus was able to enter the cell and travel to the nucleus or initiate transcription remains unclear and should be examined in future studies.

The effect that the disruption of actin filaments may have on superinfection exclusion was investigated by the use of CD. CD treatment of cells resulted in suppression of replication of the first infecting virus due to the marked delay in early gene silencing and nucleocapsid assembly in the absence of nuclear F-actin in CD-treated cells (30). Furthermore, infecting nucleocapsids are able to reach the nucleus in the absence of cytoplasmic actin, although the efficiency of this process is greatly reduced (28). When CD was removed and the second virus was inoculated, both viruses proceeded to replicate normally. This confirms the key role of nuclear actin in the replication of baculoviruses; indeed, these are the only viruses that are capable of redistributing cellular actin to the nucleus to facilitate gene expression and nucleocapsid formation (28).

Our results also show that superinfection exclusion involves not only homologous interference, but also exclusion of other lepidopteran-specific alphabaculoviruses, as every member of the genus follows the same general infection process (24). The fact that both AcMNPV and SfMNPV, two phylogenetically distant nucleopolyhedroviruses, are able to exclude superinfecting viruses suggests that this process is common to every alphabaculovirus and is likely to be mediated by one or more of the 62 open reading frames (ORFs) that have homologs in all lepidopteran-specific baculoviruses (50).

Inoculation of Sf9 cells with SfMNPV was markedly more efficient than inoculation with AcMNPV during coinfection studies. In simultaneous infections with both viruses, a lower than expected frequency of dual infections was observed (3.8% instead of 12.2% dual infections). The overall prevalence of infection was also lower than expected given an MOI of 10, suggesting that a fraction of the cells were not susceptible to infection at the moment of inoculation, despite our efforts to synchronize the cell cycle phase. Although our methodology determined the success of the virus cycle rather than specific phases of infection and replication in the dually infected cell, it was clear that the viruses interfered with one another, resulting in a lower than expected incidence of coinfection. It is not clear at present which aspects of the virus-cell relationship are involved in this interaction. However, our results clearly demonstrate that productive coinfection with two phylogenetically distant nucleopolyhedroviruses can occur.

In conclusion, the results presented here suggest that superinfection exclusion is likely to be common in alphabaculovirus-infected cells. Furthermore, disruption of actin filaments in the cells by treatment with cytochalasin D inhibited the exclusion process. The closing of the temporal window of superinfection coincided with the reorganization of cytoplasmic actin to F-actin in the nucleus, which in turn coincided with the end of the early phase of infection (12 to 15 h p.i.). The temporal window of susceptibility to subsequent virus infection, during which multiple budded virions can infect cells, is likely necessary to promote genotypic diversity that favors the transmission and survival of alphabaculoviruses but incidentally allows defective genotypes (44, 51) and heterologous alphabaculoviruses to coinfect these cells. These findings also point to a possible mechanism that facilitates recombination between homologous and heterologous baculoviruses within dually infected insects. This mechanisms' potential to generate novel genotypes that comprise mosaics of genes from phylogenetically distant origins is an intriguing one that merits consideration during studies on baculovirus evolution and the phylogenetic relationships within this family of viruses.

ACKNOWLEDGMENTS

We thank C. M. Griffiths and J. O. Danquah (Oxford Brookes University) for providing viruses and technical assistance.

I.B. received a CSIC studentship. This research was supported by the project AGL2011-30352-CO2-01 (Universidad Pública de Navarra, Pamplona, Spain) and Oxford Brookes University, Oxford, United Kingdom.

REFERENCES

1. **Ellenberg P, Linero FN, Scolaro LA.** 2007. Superinfection exclusion in BHK-21 cells persistently infected with Junín virus. J. Gen. Virol. **88:** 2730–2739. http://dx.doi.org/10.1099/vir.0.83041-0.
2. **Lee YM, Tscherne DM, Yun SI, Frolov I, Rice CM.** 2005. Dual mechanisms of pestiviral superinfection exclusion at entry and RNA replication. J. Virol. **79:**3231–3242. http://dx.doi.org/10.1128/JVI.79.6.3231-3242.2005.
3. **Tscherne DM, Evans MJ, von Hahn T, Jones CT, Stamataki Z, McKeating JA, Lindenbach BD, Rice CM.** 2007. Superinfection exclusion in cells infected with hepatitis C virus. J. Virol. **81:**3693–3703. http://dx.doi.org/10.1128/JVI.01748-06.
4. **Folimonova SY.** 2012. Superinfection exclusion is an active virus-controlled function that requires a specific viral protein. J. Virol. **86:**5554–5561. http://dx.doi.org/10.1128/JVI.00310-12.
5. **Folimonova SY, Robertson CJ, Shilts T, Folimonov AS, Hilf ME, Garnsey SM, Dawson WO.** 2010. Infection with strains of *Citrus Tristeza Virus* does not exclude superinfection by other strains of the virus. J. Virol. **84:**1314–1325. http://dx.doi.org/10.1128/JVI.02075-09.
6. **Nethe M, Berkhout B, van der Kuyl A.** 2005. Retroviral superinfection resistance. Retrovirology **2:**52. http://dx.doi.org/10.1186/1742-4690-2-52.
7. **Schaller T, Appel N, Koutsoudakis G, Kallis S, Lohmann V, Pietschmann T, Bartenschlager R.** 2007. Analysis of hepatitis C virus superinfection exclusion by using novel fluorochrome gene-tagged viral genomes. J. Virol. **81:**4591–4603. http://dx.doi.org/10.1128/JVI.02144-06.
8. **Simon KO, Cardamone JJ, Whitaker-Dowling PA, Youngner JS, Widnell CC.** 1990. Cellular mechanisms in the superinfection exclusion of vesicular stomatitis virus. Virology **177:**375–379. http://dx.doi.org/10.1016/0042-6822(90)90494-C.
9. **Salem T, Cheng X-H, Cheng X-W.** 2012. AcMNPV enhances infection by ThorNPV in Sf21 cells and SeMNPV in Hi5 cells. Arch. Virol. **157:**1875–1885. http://dx.doi.org/10.1007/s00705-012-1347-2.
10. **Weng Q, Yang K, Xiao W, Yuan M, Zhang W, Pang Y.** 2009. Establishment of an insect cell clone that harbours a partial baculoviral genome

and is resistant to homologous virus infection. J. Gen. Virol. **90:**2871–2876. http://dx.doi.org/10.1099/vir.0.013334-0.
11. **Xu X, Chen Y, Zhao Y, Liu X, Dong B, Jones IM, Chen H.** 2013. Baculovirus superinfection: a probable restriction factor on the surface display of proteins for library screening. PLoS One **8:**e54631. http://dx.doi.org/10.1371/journal.pone.0054631.
12. **Moscardi F.** 1999. Assessment of the application of baculoviruses for control of Lepidoptera. Annu. Rev. Entomol. **44:**257–289. http://dx.doi.org/10.1146/annurev.ento.44.1.257.
13. **Hitchman RB, Locanto E, Possee RD, King LA.** 2011. Optimizing the baculovirus expression vector system. Methods **55:**52–57. http://dx.doi.org/10.1016/j.ymeth.2011.06.011.
14. **Kost TA, Condreay JP, Jarvis DL.** 2005. Baculovirus as versatile vectors for protein expression in insect and mammalian cells. Nat. Biotechnol. **23:**567–575. http://dx.doi.org/10.1038/nbt1095.
15. **Szewczyk B, Hoyos-Carvajal L, Paluszek M, Skrzecz I, Lobo de Souza M.** 2006. Baculoviruses: re-emerging biopesticides. Biotechnol. Adv. **24:**143–160. http://dx.doi.org/10.1016/j.biotechadv.2005.09.001.
16. **van Oers MM.** 2011. Opportunities and challenges for the baculovirus expression system. J. Invertebr. Pathol. **107:**S3–S15. http://dx.doi.org/10.1016/j.jip.2011.05.001.
17. **Safdar A, Cox MM.** 2007. Baculovirus-expressed influenza vaccine. A novel technology for safe and expeditious vaccine production for human use. Expert Opin. Investig. Drugs **16:**927–934. http://dx.doi.org/10.1517/13543784.16.7.927.
18. **van Oers MM.** 2006. Vaccines for viral and parasitic diseases produced with baculovirus vectors. Adv. Virus Res. **68:**193–253. http://dx.doi.org/10.1016/S0065-3527(06)68006-8.
19. **Chen CY, Lin CY, Chen GY, Hu YC.** 2011. Baculovirus as a gene delivery vector: recent understandings of molecular alterations in transduced cells and latest applications. Biotechnol. Adv. **29:**618–631. http://dx.doi.org/10.1016/j.biotechadv.2011.04.004.
20. **Peng K, van Lent JWM, Boeren S, Fang M, Theilmann DA, Erlandson MA, Vlak JM, van Oers MM.** 2012. Characterization of novel components of the baculovirus *per os* infectivity factor (PIF) complex. J. Virol. **86:**4981–4988. http://dx.doi.org/10.1128/JVI.06801-11.
21. **Peng K, van Oers MM, Hu Z, van Lent JWM, Vlak JM.** 2010. Baculovirus *per os* infectivity factors form a complex on the surface of occlusion-derived virus. J. Virol. **84:**9497–9504. http://dx.doi.org/10.1128/JVI.00812-10.
22. **Long G, Pan X, Kormelink R, Vlak JM.** 2006. Functional entry of baculovirus into insect and mammalian cells is dependent on clathrin-mediated endocytosis. J. Virol. **80:**8830–8833. http://dx.doi.org/10.1128/JVI.00880-06.
23. **Ohkawa T, Volkman LE, Welch MD.** 2010. Actin-based motility drives baculovirus transit to the nucleus and cell surface. J. Cell Biol. **190:**187–195. http://dx.doi.org/10.1083/jcb.201001162.
24. **Rohrmann GF.** 2008. Baculovirus molecular biology. National Library of Medicine, Bethesda, MD.
25. **Danquah JO, Botchway S, Jeshtadi A, King LA.** 2012. Direct interaction of baculovirus capsid proteins VP39 and EXON0 with kinesin-1 in insect cells determined by fluorescence resonance energy transfer-fluorescence lifetime imaging microscopy. J. Virol. **86:**844–853. http://dx.doi.org/10.1128/JVI.06109-11.
26. **Fang M, Nie Y, Theilmann DA.** 2009. AcMNPV EXON0 (AC141) which is required for the efficient egress of budded virus nucleocapsids interacts with β-tubulin. Virology **385:**496–504. http://dx.doi.org/10.1016/j.virol.2008.12.023.
27. **Gandhi KM, Ohkawa T, Welch MD, Volkman LE.** 2012. Nuclear localization of actin requires AC102 in *Autographa californica* multiple nucleopolyhedrovirus-infected cells. J. Gen. Virol. **93:**1795–1803. http://dx.doi.org/10.1099/vir.0.041848-0.
28. **Volkman LE.** 2007. Baculovirus infectivity and the actin cytoskeleton. Curr. Drug Targets **8:**1075–1083. http://dx.doi.org/10.2174/138945007782151379.
29. **Talhouk SN, Volkman LE.** 1991. *Autographa californica* M nuclear polyhedrosis virus and cytochalasin D: antagonists in the regulation of protein synthesis. Virology **182:**626–634. http://dx.doi.org/10.1016/0042-6822(91)90603-9.
30. **Volkman LE, Talhouk SN, Oppenheimer DI, Charlton CA.** 1992. Nuclear F-actin: a functional component of baculovirus-infected lepidopteran cells? J. Cell Sci. **103:**15–22.
31. **Jehle JA, Lange M, Wang H, Hu Z, Wang Y, Hauschild R.** 2006. Molecular identification and phylogenetic analysis of baculoviruses from Lepidoptera. Virology **346:**180–193. http://dx.doi.org/10.1016/j.virol.2005.10.032.
32. **King LA, Possee R.** 1992. The baculovirus expression system. A laboratory guide. Chapman & Hall, London, United Kingdom.
33. **Ayres MD, Howard SC, Kuzio J, López-Ferber M, Possee RD.** 1994. The complete DNA sequence of *Autographa californica* nuclear polyhedrosis virus. Virology **202:**586–605. http://dx.doi.org/10.1006/viro.1994.1380.
34. **Simón O, Palma L, Beperet I, Muñoz D, López-Ferber M, Caballero P, Williams T.** 2011. Sequence comparison between three geographically distinct *Spodoptera frugiperda* multiple nucleopolyhedrovirus isolates: detecting positively selected genes. J. Invertebr. Pathol. **107:**33–42. http://dx.doi.org/10.1016/j.jip.2011.01.002.
35. **Francis B, Green M, Payne C.** 1993. *In* Francis B, Green M, Payne C (ed),. The GLIM system: release 4 manual. Clarendon Press, Oxford, United Kingdom.
36. **Wu SC, Jarvis DL, Dale BE, Liao JC.** 1994. Heterologous protein expression affects the death kinetics of baculovirus-infected insect cell cultures: a quantitative study by use of n-target theory. Biotechnol. Prog. **10:**55–59. http://dx.doi.org/10.1021/bp00025a006.
37. **Kadlec J, Loureiro S, Abrescia NG, Stuart DI, Jones IM.** 2008. The postfusion structure of baculovirus gp64 supports a unified view of viral fusion machines. Nat. Struct. Mol. Biol. **15:**1024–1030. http://dx.doi.org/10.1038/nsmb.1484.
38. **Westenberg M, Uijtdewilligen P, Vlak JM.** 2007. Baculovirus envelope fusion proteins F and GP64 exploit distinct receptors to gain entry into cultured insect cells. J. Gen. Virol. **88:**3302–3306. http://dx.doi.org/10.1099/vir.0.83240-0.
39. **Westenberg M, Vlak JM.** 2008. GP64 of group I nucleopolyhedroviruses cannot readily rescue infectivity of group II f-null nucleopolyhedroviruses. J. Gen. Virol. **89:**424–431. http://dx.doi.org/10.1099/vir.0.83342-0.
40. **Wickham TJ, Granados RR, Wood HA, Hammer DA, Shuler ML.** 1990. General analysis of receptor-mediated viral attachment to cell surfaces. Biophys. J. **58:**1501–1516. http://dx.doi.org/10.1016/S0006-3495(90)82495-4.
41. **Bull JC, Godfray HCJ, O'Reilly DR.** 2001. Persistence of an occlusion-negative recombinant nucleopolyhedrovirus in *Trichoplusia ni* indicates high multiplicity of cellular infection. Appl. Environ. Microbiol. **67:**5204–5209. http://dx.doi.org/10.1128/AEM.67.11.5204-5209.2001.
42. **Clavijo G, Williams T, Muñoz D, Caballero P, Lopez-Ferber M.** 2010. Mixed genotype transmission bodies and virions contribute to the maintenance of diversity in an insect virus. Proc. R. Soc. B. **277:**943–951. http://dx.doi.org/10.1098/rspb.2009.1838.
43. **Cory JS, Myers JH.** 2003. The ecology and evolution of insect baculoviruses. Annu. Rev. Ecol. Evol. Syst. **34:**239–272. http://dx.doi.org/10.1146/annurev.ecolsys.34.011802.132402.
44. **López-Ferber M, Simón O, Williams T, Caballero P.** 2003. Defective or effective? Mutualistic interactions between virus genotypes. Proc. R. Soc. B. **270:**2249–2255. http://dx.doi.org/10.1098/rspb.2003.2498.
45. **Huh NE, Weaver RF.** 1990. Identifying the RNA-polymerases that synthesize specific transcripts of the *Autographa californica* nuclear polyhedrosis virus. J. Gen. Virol. **71:**195–201. http://dx.doi.org/10.1099/0022-1317-71-1-195.
46. **Passarelli AL, Guarino LA.** 2007. Baculovirus late and very late gene regulation. Curr. Drug Targets **8:**1103–1115. http://dx.doi.org/10.2174/138945007782151324.
47. **Charlton CA, Volkman LE.** 1991. Sequential rearrangement and nuclear polymerization of actin in baculovirus-infected *Spodoptera frugiperda* cells. J. Virol. **65:**1219–1227.
48. **Dreschers S, Roncarati R, Knebel-Morsdorf D.** 2001. Actin rearrangement-inducing factor of baculoviruses is tyrosine phosphorylated and co-localizes to F-actin at the plasma membrane. J. Virol. **75:**3771–3778. http://dx.doi.org/10.1128/JVI.75.8.3771-3778.2001.
49. **Roncarati R, Knebel-Morsdorf D.** 1997. Identification of the early actin-rearrangement-inducing factor gene, arif-1, from *Autographa californica* multicapsid nuclear polyhedrosis virus. J. Virol. **71:**7933–7941.
50. **Jehle JA, Blissard GW, Bonning BC, Cory JS, Herniou EA, Rohrmann GF, Theilmann DA, Thiem SM, Vlak JM.** 2006. On the classification and nomenclature of baculoviruses: a proposal for revision. Arch. Virol. **151:**1257–1266. http://dx.doi.org/10.1007/s00705-006-0763-6.
51. **Muñoz D, Caballero P.** 2000. Persistence and effects of parasitic genotypes in a mixed population of the *Spodoptera exigua* nucleopolyhedrovirus. Biol. Control **19:**259–264. http://dx.doi.org/10.1006/bcon.2000.0864.